Cu Nanoparticles Have Different Impacts in *Escherichia coli* and *Lactobacillus brevis* than Their Microsized and Ionic Analogues

Chitrada Kaweeteerawat,[†,‡,§,⊥] Chong Hyun Chang,[†,‡] Kevin R. Roy,[∥] Rong Liu,[†,‡,#] Ruibin Li,[†,‡] Daniel Toso,[▽] Heidi Fischer,[○] Angela Ivask,[†,‡,⊗,△] Zhaoxia Ji,[†,‡] Jeffrey I. Zink,[†,‡,◆] Z. Hong Zhou,[‡,×] Guillaume Francois Chanfreau,[∥] Donatello Telesca,[†,‡,○] Yoram Cohen,[†,‡,#,◇] Patricia Ann Holden,[†,+] Andre E. Nel,[†,‡,¶] and Hilary A. Godwin[*,†,‡,§,⊥,#]

[†]University of California Center for Environmental Implications of Nanotechnology, University of California, Los Angeles, California 90095, United States, [‡]California NanoSystems Institute, University of California, Los Angeles, California 90095, United States, [§]Molecular Toxicology Interdepartmental Degree Program, University of California, Los Angeles, California 90095, United States, [⊥]Department of Environmental Health Sciences, Fielding School of Public Health, University of California, Los Angeles, California 90095, United States, [∥]Department of Chemistry and Biochemistry and the Molecular Biology Institute, University of California, Los Angeles, California 90095, United States, [#]Institute of the Environment and Sustainability, University of California, Los Angeles, California 90039, United States, [▽]Biomedical Engineering Interdepartmental Program, University of California, Los Angeles, California 90095, United States, [○]Department of Biostatistics, Fielding School of Public Health, University of California, Los Angeles (UCLA), Los Angeles, California 90095, United States, [⊗]Laboratory of Environmental Toxicology, National Institute of Chemical Physics and Biophysics, Tallinn, 12618, Estonia, [◆]Department of Chemistry and Biochemistry, University of California, Los Angeles, California 90095, United States, [×]Department of Microbiology, Immunology, and Molecular Genetics, University of California, Los Angeles, California 90095, United States, [◇]Department of Chemical and Biomolecular Engineering, University of California, Los Angeles, California 90095, United States, [+]Bren School of Environmental Science and Management, University of California, and Earth Research Institute, Santa Barbara, California 93106, United States, and [¶]Division of NanoMedicine, Department of Medicine, University of California, Los Angeles, California 90095, United States. [△]Present address: Mawson Institute, University of South Australia, Mawson Lakes 5095, Australia.

ABSTRACT Copper formulations have been used for decades for antimicrobial and antifouling applications. With the development of nanoformulations of copper that are more effective than their ionic and microsized analogues, a key regulatory question is whether these materials should be treated as new or existing materials. To address this issue, here we compare the magnitude and mechanisms of toxicity of a series of Cu species (at concentration ranging from 2 to 250 μg/mL), including nano Cu, nano CuO, nano $Cu(OH)_2$ (CuPro and Kocide), micro Cu, micro CuO, ionic Cu^{2+} ($CuCl_2$ and $CuSO_4$) in two species of bacteria (*Escherichia coli* and *Lactobacillus brevis*). The primary size of the particles studied ranged from 10 nm to 10 μm. Our results reveal that Cu and CuO nanoparticles (NPs) are more toxic than their microsized counterparts at the same Cu concentration, with toxicities approaching those of the ionic Cu species. Strikingly, these NPs showed distinct differences in their mode of toxicity when compared to the ionic and microsized Cu, highlighting the unique toxicity properties of materials at the nanoscale. *In vitro* DNA damage assays reveal that both nano Cu and microsized Cu are capable of causing complete degradation of plasmid DNA, but electron tomography results show that only nanoformulations of Cu are internalized as intact intracellular particles. These studies suggest that nano Cu at the concentration of 50 μg/mL may have unique genotoxicity in bacteria compared to ionic and microsized Cu.

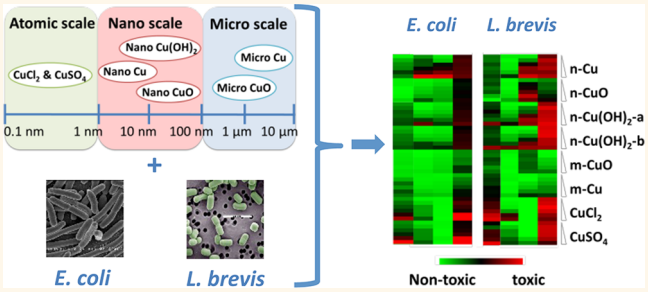

KEYWORDS: copper · nanoparticle · nanotoxicology · ecotoxity · antimicrobial · antifouling · genotoxicity

Nanomaterials have contributed to rapid advances in diverse fields including engineering, materials development, medicine, and energy conservation, as well as space technology.[1] For nano-enabled products to be brought to market and have a sustainable future, we need to understand their toxicity and ecotoxicity. Here, we have chosen to focus on nanoformulations of Cu, which are used as lubricants, conducting polymers, surfactants, and catalysts in chemical reactions,[2,3] as well as drugs, deodorants, food additives, and as antifouling agents in paint.[4,5] Nanoformulations of Cu that are used commercially in environmental settings include nano

* Address correspondence to hgodwin@ucla.edu.

Received for review April 3, 2015 and accepted July 7, 2015.

Published online July 13, 2015
10.1021/acsnano.5b02021

$Cu(OH)_2$ (*e.g.*, CuPro and Kocide), nano CuO (n-CuO) and nano Cu (n-Cu). Many of the current and proposed applications for these materials take advantage of the potent antibacterial properties of Cu species. However, because of their antibacterial properties, Cu-based nanoparticles (Cu NPs) may also have unwanted effects in ecosystems. A central question is whether the magnitude and/or mechanisms of toxicity of Cu-based nanoparticles are the same as, or different from, those of other traditional Cu formulations that are already on the market.

Cu-based nanoparticles have been shown to exhibit toxicity against a wide range of environmentally relevant organisms. For example, CuO nanoparticles have been shown to induce growth inhibition and lead to cellular oxidative stress in green alga,[6] compromise the health of daphnia,[7] and lead to neurotoxic effects in mussels[8] at the no observed effect level (NOEL) less than 100, 0.8, and 0.01 mg/L respectively. Moreover, Cu nanoparticles have also been shown to cause gill injury and acute lethality in zebrafish with an LD_{50} at 48 h of 1.5 mg/L.[9] In the bacterium *Escherichia coli*, CuO nanoparticles have been shown to induce cytotoxicity and oxidative stress with an LD_{50} at 30 min of 0.16 mg/L.[10] There is also evidence to suggest that Cu-based nanoparticles may pose a threat to human health: CuO NPs were found to cause acute pulmonary inflammation at 1 mg/kg when oropharyngeally administrated in mice and lethality in human mesenchymal stem cells with an IC_{50} value of 2.5 μg/mL.[11,12]

To address the question of whether the toxicity of nanoparticles is unique, it is critical to conduct direct comparisons between nanoparticles and their ionic and microsized counterparts under comparable conditions. For metallic nanoparticles, some researchers have suggested that the toxicity of the nanoparticles is due to dissolved metal ions, and hence, metal nanoparticles simply constitute a novel delivery mechanism for an existing agent.[13] For instance, Alvarez and coworkers reported that the toxicity of silver nanoparticles corresponds to the rate of the release of silver ions into solution, and that no particle-specific effects were observed when conducting the experiments in a completely anaerobic condition in bacteria.[13] By contrast, other studies have shown that some (but not all) Ag nanoparticles exhibit mechanisms of toxicity that are different from their ionic analogues. For instance, studies comparing the toxicity of various Ag NPs with ionic Ag^+ using microarray analysis[14] and genome-wide single gene deletion mutants in *E. coli*[15] revealed that the pathways involved in the response of this bacterium are distinct for different Ag NPs and vary from those seen for Ag^+. In the gene deletion strain studies, the toxicity of Ag-BPEI, which is a cationic Ag NP, was shown to involve pathways similar to those of $PS\text{-}NH_2$, a cationic NP that contains no Ag^+.[15] Moreover, in erythroid (mammalian) cells, silver nanoparticles have been found to disrupt transcription by inhibiting RNA polymerase, a process that was distinctly different from cytotoxic pathways induced by silver ions.[16]

Similarly, reports as to whether Cu nanoparticles are toxic simply because they release Cu ions or whether they can exhibit nanospecific toxicity have been a subject of debate in the literature. Bondarenko and co-workers have reported toxicity studies comparing nano CuO to $CuSO_4$ and microsized CuO at the exposure concentration of 0.001−10000 mg/L in *E. coli*.[17] On the basis of their results, they suggested that nano CuO was toxic due to the copper ion released into solution because all three copper species resulted in biotic production of reactive oxygen species (ROS) and single-stranded DNA damage; additionally, these effects could be inhibited by addition of a Cu-chelating agent (EDTA).[17] By contrast, in a separate study of *Pseudomanas chlororaphis*, only CuO nanoparticles, but not their bulk or ionic counterparts, were found to modify bacterial metabolism and cellular reprogramming at the exposure concentration of 200 mg/L.[18] In addition, a study in the microcrustacean *Daphnia magna* and in the bacterium *Vibrio fischeri* revealed that CuO particles at the nanosize are about 10 times more toxic than their bulk analogues at the exposure concentration of 3.8−250 mg/L for *D. magna* and 0−4000 mg/L for *V. fischeri*.[19]

These somewhat conflicting results point to the need for a systematic and thorough analysis of the difference in toxicity mechanisms for multiple species of bacteria from related Cu species at the nanosize and the microsize in comparison to ionic Cu. Here, we demonstrate the use of a suite of sublethal assays consisting of membrane damage, cellular ROS generation, electron transport activity and membrane potential to unveil the molecular mechanisms of toxicity of a panel of nanoparticles (n-Cu, n-CuO and $Cu(OH)_2$) compared to their microsized analogues (m-Cu and m-CuO) as well as ionic Cu ($CuCl_2$ and $CuSO_4$). In addition, we evaluated the toxicity of the Cu species in two very different taxa of bacteria: *E. coli*, a Gram-negative bacterium, and *Lactobacillus brevis*, a Gram-positive bacterium. We intentionally selected two different species of enteric bacteria so that we could explore possible implications of Cu-based nanoparticles entering into liquid waste treatment systems that rely on microorganisms. These results have important implications for both the regulation of Cu-based nanoparticles and for the design of safer products containing Cu species.

RESULTS AND DISCUSSION

Cu Species Varied in Size from Nanoscale to Microscale. The toxic effects of the selected particles (Supporting Information Table S1) were determined in Gram-negative bacterium and Gram-positive enteric bacteria. Our material selection included Cu particles that varied

TABLE 1. Zeta Potential, Particle Size, and Hydrodynamic Diameter of Cu Particles in Purified Water and Bacterial Media[a]

			average hydrodynamic diameter (nm)[d]				
				MMD + HA[e]		Lactobacilli media	
particles	zeta potential (mV)	primary size (nm)[b]	purified water	0 h	24 h	0 h	24 h
n-Cu	−46.3 ± 1.6	200−1000	1200 ± 200	1100 ± 200	1400 ± 300	1600 ± 500	1400 ± 500
n-CuO	−16.5 ± 0.8	20−100	420 ± 20	300 ± 2	460 ± 10	470 ± 4	1600 ± 300
n-$Cu(OH)_2$-a	−45.1 ± 0.8	10	900 ± 200	270 ± 1	300 ± 10	390 ± 10	400 ± 30
n-$Cu(OH)_2$-b	−53.8 ± 0.7	N/A[c]	1400 ± 100	240 ± 2	250 ± 10	280 ± 1	290 ± 2
m-CuO	−28.5 ± 0.9	200−2000	1300 ± 200	1300 ± 500	1500 ± 600	N/A[f]	N/A[f]
m-Cu	−32.5 ± 2.9	>10,000	N/A[f]	N/A[f]	N/A[f]	N/A[f]	N/A[f]

[a] Error bars indicate standard error of measurements. [b] Primary sizes were measured by TEM, $n = 100$. [c] Primary size could not be obtained because particles are of undefined morphology. [d] Standard error was measured from three experiments. [e] HA = humic acid, which was added as a stabilizing agent. [f] N/A indicates that particles size exceeds instrumentation range (0.3 nm to 3 μm) according to the manufacturer of the Dynamic Light Scattering machine.

in size (nanoscale to microscale) as well as chemical composition (elemental Cu, CuO, and $Cu(OH)_2$). Six different Cu particulates were studied: nano Cu (n-Cu), nano CuO (n-CuO), nano $Cu(OH)_2$ (2 forms, n-$Cu(OH)_2$-a and n-$Cu(OH)_2$-b), micro Cu (m-Cu), and micro CuO (m-CuO). Because n-$Cu(OH)_2$ constitutes the most widely used class of nanosized Cu fungicide/bactericides, we tested two different commercial sources of CuPro; n-$Cu(OH)_2$-a and Kocide; n-$Cu(OH)_2$-b to determine whether there are any manufacturer-dependent differences in environmental effects for this class of Cu NPs. In addition, two different forms of ionic Cu ($CuCl_2$ and $CuSO_4$) were tested as controls. The toxic effects of these particles were determined in *E. coli* and *L. brevis*: *E. coli* is a Gram-negative bacterium and *L. brevis* is a Gram-positive bacterium.

The primary sizes (diameter) of the particles (as shown in Table 1) were less than 1000 nm for all of the nanoscale particles (n-Cu, n-CuO, n-$Cu(OH)_2$-a and n-$Cu(OH)_2$-b) and ranged from 200 nm to >10 μm for microscaled particles (m-Cu and m-CuO). It is important to note that the "nano-Cu" species was reported by the manufacturer (U.S. Research Nanomaterials) to be "40 nm".[20] However, when we looked at this sample using TEM, we found that the primary size to range between 200 and 1000 nm. Nonetheless, we have continued to refer to this sample as "nano-Cu" to be consistent with the designation given to this material in prior publications from our center, UC-CEIN.[20,21] The hydrodynamic diameter of these particles in purified water was less than 1400 nm for all of the nanoscaled particles and ranged in size between ∼1300 nm and >3 μm for the microscaled particles. When dispersed in *E. coli* minimal (MMD) media, the average hydrodynamic diameter of the particles was approximately the same as that observed in purified water (see Table 1). However, when the particles were dispersed in Lactobacilli MRS broth, the average hydrodynamic diameter was slightly larger (280−1600 nm for nanoscaled particles and >3 μm for microsized particles) than that observed in purified water. This slight increase of hydrodynamic diameter found in nutrient-rich Lactobacilli MRS broth might be the result of adsorption of proteins from the media onto the surface of the particles.[22] All of the particles remained stable in both *E. coli* and *L. brevis* media after 24 h as shown in Table 1, when dispersed using humic acid as described in the Materials and Methods. The zeta potential of the particles ranged from −16.5 to −53.8 mV in purified water (Table 1). The percentage of Cu ion dissolution from each particle in purified water, *E. coli* MMD media, and Lactobacilli media are provided in Table 2. n-Cu and the two n-$Cu(OH)_2$ nanoparticles (CuPro and Kocide) dissolved more than the rest of the particles in both bacterial media studied, but still not completely (10%, 10%, and 11% in MMD media and 21%, 22%, and 18% in Lactobacilli media after 24 h for n-Cu, n-$Cu(OH)_2$-a, and n-$Cu(OH)_2$-b, respectively). Interestingly, for all of the particles studied, the particles dissolved most in the Lactobacilli media, an intermediate amount in the MMD media, and least in purified water. This dissolution trend presumably reflects the greater ionic strength and organic materials present in Lactobacilli media > MMD media > water; increasing ionic strength and the presence of some organic species have both been shown previously to facilitate the dissolution of Cu ions from the particles.[20]

Bacteria Exhibit Differential Sensitivities to Different Cu Species, with Gram-Positive Bacteria More Sensitive than Gram-Negative Bacteria. To study the antibacterial effects of Cu particles, growth inhibition assays were performed on both *E. coli* and *L. brevis*. Dose-dependent declines in bacterial growth were observed for all of the Cu species tested in both species of bacteria (Supporting Information Figure S1A, *E. coli*; B, *L. brevis* and Supporting Information Figure S2 showing individual growth-inhibition curves with error bars for each of the Cu species in *E. coli* (A) and *L. brevis* (B)), but the magnitude of the toxicity (as measured by IC_{50}) differed significantly between the Cu species studied and between the two

TABLE 2. IC_{50} Values, % Cu Ion Dissolution, Amount of Cell-Associated Cu by Sucrose Gradient Centrifugation, and % Cu Bioavailable by Biosensor Stain for Different Cu Species and Different Bacteria Studied Herein[a]

			%Cu ion dissolution *in vitro*			Cu associated with cells by sucrose gradient centrifugation (ppm/10^9 cells)		
NPs	*E. coli* IC_{50} (μg/mL)	*L. brevis* IC_{50} (μg/mL)	water	*E. coli* (MMD) media	*L. brevis* MRS media	*E. coli* (1 mg/mL)	*L. brevis* (1 mg/mL)	% Cu bioavailable (*E. coli* biosensor)
$CuCl_2$	38 ± 8	7.8 ± 0.5	100	100	100	N/A[b]	N/A[b]	100
$CuSO_4$	140 ± 23	24 ± 3	100	100	100	N/A[b]	N/A[b]	-
n-Cu	120 ± 14	5.7 ± 0.2	0.1 ± 0.0	9.9 ± 0.4	20.7 ± 0.4	10.4 ± 0.1	10.5 ± 0.3	100
n-CuO	160 ± 17	3.6 ± 0.1	0.0 ± 0.0	7.5 ± 0.1	10.9 ± 0.1	4.3 ± 0.1	3.9 ± 0.1	70
n-$Cu(OH)_2$-a	>250	4.0 ± 0.1	2.7 ± 0.1	9.9 ± 0.6	21.8 ± 0.6	8.3 ± 0.3	5.4 ± 0.1	17.5
n-$Cu(OH)_2$-b	>250	6.2 ± 0.9	5.4 ± 0.2	10.8 ± 0.6	17.9 ± 0.6	8.0 ± 0.4	5.6 ± 0.1	-
m-CuO	>250	>250	0.0 ± 0.0	2.9 ± 0.3	3.3 ± 0.3	1.2 ± 0.0	0.9 ± 0.0	4.4
m-Cu	>250	120 ± 24	0.1 ± 0.0	2.1 ± 0.8	5.6 ± 0.8	0.4 ± 0.0	1.5 ± 0.1	10.9

[a] Error bars represent standard deviation of measurements. [b] NA = not applicable, because it was not possible to separate ionic Cu from bacterial cells using sucrose gradient centrifugation.

species of bacteria (Table 2). Markedly, a severe interruption of growth was observed when *E. coli* was treated with $CuCl_2$, n-Cu, $CuSO_4$, and n-CuO (the IC_{50} was determined to be 38, 120, 140, and 160 mg/L for these species, respectively, Table 2). The observed difference in toxicity between $CuCl_2$ and $CuSO_4$ agrees with the previously published data showing the distinct behaviors in bioreduction and biosorption between the two Cu compounds[23] and the influence of chloride and sulfate anions on the bioavailability of Cu and subsequently the uptake of Cu into starch granules in potato and wheat starch.[24] A relatively mild response ($IC_{50} \geq$ 250 mg/L) was observed when *E. coli* was treated with n-$Cu(OH)_2$-a and n-$Cu(OH)_2$-b as well as microsized particles (m-Cu and m-CuO). Notably, *L. brevis* was more sensitive (as indicated by a smaller IC_{50} value) to each of the Cu species tested than was *E. coli*. n-CuO, n-$Cu(OH)_2$-a, n-Cu, n-$Cu(OH)_2$-b, and $CuCl_2$ exhibited IC_{50} values of 4, 4, 6, 6, and 8, respectively, in *L. brevis*, which meets the criteria for "toxic to aquatic life" according to the globally harmonized system of classification and labeling of chemicals (GHS) part 4: Environmental hazard.[25] A relatively modest response ($IC_{50} \geq$ 120 mg/L) was observed in *L. brevis* for m-Cu and m-CuO (Supporting Information Figures S1 and S2 and Table 2). To accurately distinguish between toxic and nontoxic Cu species, the area under the growth inhibition curves (as shown in Supporting Information Figure S1) was calculated for all of the Cu species (Supporting Information Figure S3). The calculation provided a continuous measurement for nontoxic particles whose exact IC_{50} could not be determined. (Note that the IC_{50} of these nontoxic particles was listed as ≥250 mg/mL in Table 2). In agreement with the IC_{50} values, nanosized particles and ionic Cu exhibit a significantly smaller area under their respective growth inhibition curves when compared to their microsized particles in both species of bacteria confirming that the nanosized Cu particles are more toxic than their microsized counterparts. In both species of bacteria, the toxicity of the n-Cu was equivalent to that of toxic ionic Cu species ($CuCl_2$, $CuSO_4$, Table 2, Supporting Information Figure S3). Interestingly, the Gram-positive *L. brevis* exhibited an elevated toxicity to all of the particles relative to Gram-negative *E. coli*, suggesting a possible role for the double membrane structure found specifically in Gram-negative bacteria in protecting against toxicity of Cu particles. However, it is important to note that toxicity assays in the two bacterial species were conducted in two different types of media: MMD for *E. coli* and MRS media for *L. brevis*. Metal ion dissolution was found to be significantly higher in the MRS media, suggesting that the increased sensitivity of *L. brevis* toward Cu species could be partially due to elevated dissolved Cu ions in *L. brevis* media compared to *E. coli* media. To address this issue, we performed a regression analysis of the area under the growth inhibition curve as a function of the concentration of Cu dissolved in the bacterial media where data for both *E. coli* and *L. brevis* were considered both separately and together (Supporting Information Figure S4). This analysis reveals that the regression lines for the two species are quite similar but not identical, suggesting that the difference in toxicity observed in the two species may be largely (but not completely) due to differences in the extent of the dissolution of the copper species in the media. However, the observation that *L. brevis* is more sensitive than *E. coli* is also consistent with the previous finding that Gram-positive bacteria are more sensitive to nanoparticles compared to Gram-negative counterpart in the case of CuO nanoparticles and nanosized metal oxide halogen adducts[26,27] and that Gram-positive bacteria tend to be more sensitive than Gram-negative bacteria to ionic copper and other metal ions.[28,29]

Magnitude of Toxicity of Cu Species Correlates with Amount of Cell-Associated Copper. One possible explanation for

why bacteria are more sensitive to nanosized copper species than to microsized copper species was proposed previously by Rossetto *et al.*, *i.e.*, that the percent dissolution of the nano copper species is greater than for microsized Cu species due to the larger surface to volume ratio for nanosized particles.[19] To test this possibility, we looked at whether the area under the growth inhibition curve for the different Cu species correlates with the amount of dissolved Cu in the bacterial media. The area under the dose−response curve was determined to provide a continuous measure of toxicity, which is necessary because the IC_{50} could not be determined exactly for the nontoxic species (*i.e.*, those Cu species where $IC_{50} \geq 250$ mg/L). The correlation between area under the growth inhibition curve and the amount of Cu dissolved in the bacterial media was found to be moderate for *E. coli* ($r = 0.65$) and strong for *L. brevis* ($r = 0.83$) (see Supporting Information Table S2).[30]

Because we had recently observed that the toxicity of silver nanoparticles is dependent upon their ability to bind to the outside of cells and perturb the outer membrane,[15] we also tested whether the nano Cu species were more toxic because they were better able to bind to and deliver Cu to the bacterial cells. To assess this, we used sucrose gradient centrifugation coupled with ICP-OES to determine the concentration of Cu associated with bacteria. A detailed schematic of this experiment is shown in Supporting Information Figure S5. The total number of bacterial cells collected from the sucrose gradient was determined using a linear equation derived from a standard curve relating OD_{600} and total number of cells (colony forming units) as shown in Supporting Information Figure S6. Generally, there was more Cu associated with cells exposed to the more toxic Cu species than for the cells exposed to the less toxic Cu species (Table 2). In particular, n-Cu, with the smallest IC_{50} value, exhibited the greatest amount of cell-associated Cu, both in *L. brevis* and *E. coli*. The correlation between the area under the growth inhibition curves and the Cu associated with the cells was found to be 0.73 and 0.74 for *E. coli* and *L. brevis*, respectively (Supporting Information Table S2). This correlation is roughly equivalent to that observed between area under the growth inhibition curves and the amount of Cu dissolved in the bacterial media (0.65 and 0.83 for *E. coli* and *L. brevis*, respectively). One caveat to the sucrose gradient separation is that ionic Cu cannot be effectively separated from the cellular components, and hence, this method cannot be used to ascertain cell-associated Cu for bacteria treated with ionic Cu. However, these results suggest that the ability of the Cu species to associate with cells may play a crucial role in determining their toxicity and suggests the need for more detailed studies on the different mechanisms of toxicity for the Cu species.

To test whether the most important factor in determining toxicity was the amount of Cu *delivered to the inside* of the cells, we used a genetically engineered bacterial biosensor, *E. coli* MC1061 (pSLcueR/pDNPcopAlux), in which bioluminescence is specifically induced by *intracellular, bioavailable* Cu.[17] The copper species that were found to be most toxic to cells (*i.e.*, $CuCl_2$ and nanosized Cu particles) resulted in more bioluminescence than the less toxic particles (*i.e.*, microsized particles) (see Supporting Information Figure S7). The level of bioavailable Cu for cells treated with n-Cu was about the same or higher than that of cells treated with $CuCl_2$, suggesting that the nanoparticle form of Cu has a unique advantage over Cu ions in entering the cells and that particles at nanoscale are more effective in Cu ion delivery than particles at microscale. The correlation coefficient between area under the growth inhibition curve and the intracellular amount of bioavailable Cu was very strong ($r = 0.98$, Supporting Information Table S2) suggesting that the best predictor of bacterial toxicity is the amount of intracellular, bioavailable Cu.

Sublethal Assays Reveal That Different Cu Species Exhibit Different Mechanisms of Toxicity. To elucidate the mechanisms of toxicity for the Cu species, a suite of assays measuring membrane potential, membrane damage, cellular ROS generation, and electron transport activity were employed in both *E. coli* and *L. brevis*. A detailed description of these methods is also provided in the Supplemental Materials and Methods section within the Supporting Information. The outcomes of these four assays are shown in the heat map in Figure 1. In the heat map, red indicates that the results are similar to the positive control (*i.e.*, NaN_3 for the membrane potential assay, ethanol for membrane damage, H_2O_2 for cellular ROS generation, and CCCP for electron transport activity), and green indicates that the results are identical to the negative controls (*i.e.*, PBS with no added Cu species). While both nanosized Cu and Cu ions resulted in significant membrane damage and a decrease in electron transport activity in *E. coli*, the microsized Cu particles did not. This observation strongly agrees with the growth inhibition results, in which nanosized Cu and Cu ions exhibit lower IC_{50} values and smaller areas under the growth inhibition curve than the microsized Cu species in *E. coli* (Table 2, Supporting Information Figure S3). Strikingly, oxidative stress (measured by biotic ROS generation) was only observed in *E. coli* treated with Cu NPs, but not in *E. coli* treated with ionic copper ($CuCl_2$ or $CuSO_4$) or microsized Cu at the concentrations studied herein. Conversely, severe disruption of membrane potential was observed only in *E. coli* treated with Cu ions and not those treated with nano- or microsized Cu particles. In both species, the toxicity of the Cu species (as measured by area under the growth curve) was strongly correlated with the decrease in electron transport

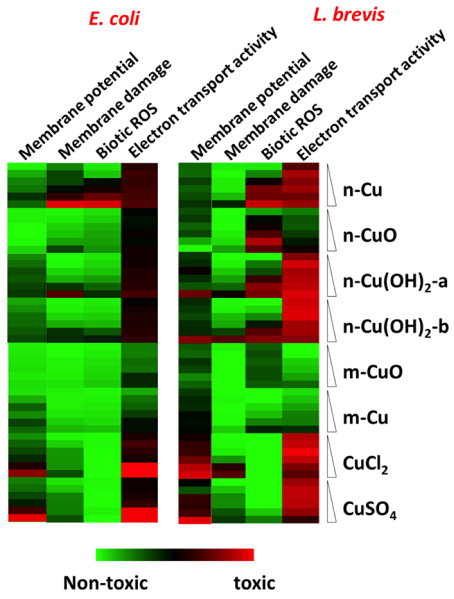

Figure 1. A suite of sublethal assays was used to elucidate the mechanisms of toxicity of the Cu species. Cells were treated with Cu particles ranging from 2 to 250 mg/L for 24 h before being treated with DiBAC, PI/SYTO, H_2DCFDA, or XTT to assess membrane potential, membrane damage, biotic ROS generation, or electron transport chain activity, respectively. Red indicates similarity for each treatment to the positive controls (NaN_3, ethanol, H_2O_2, and CCCP for membrane potential, membrane damage, cellular ROS generation, and electron transport activity assays, respectively), whereas green indicates the degree of similarity for each treatment to the negative controls (PBS alone). At least three biological replicates were performed at each concentration for each assay.

activity (correlation coefficient = 0.76 in *E. coli*, Supporting Information Table S3A and 0.64 in *L. brevis*, Table S3B). Similar trends were observed in *L. brevis* (Figure 1), with the following exceptions: (1) overall, a stronger response was observed in the sublethal assays in *L. brevis* for the more toxic particles; (2) significant membrane damage was observed for both $Cu(OH)_2$ (CuPro and Kocide) and $CuCl_2$/$CuSO_4$ in *L. brevis*; and (3) biotic ROS generation was observed in *L. brevis* treated with n-Cu and n-CuO, as well as both of the $Cu(OH)_2$ species (CuPro and Kocide). Interspecies correlation (Supporting Information Table S3C) revealed that a strong agreement between the two species was observed in biotic ROS generation (r = 0.90) and membrane potential (r = 0.86). Consistent with the results from the growth inhibition assay, however, we typically observed stronger responses in *L. brevis* than in *E. coli* for a given Cu species for each of the assays. The observation that overall toxicity does not correlate strongly with biotic ROS generation for the series of copper species (r = 0.02 in *E. coli* and r = 0.60 in *L.* brevis) is important because it suggests that different toxicity mechanisms are relevant to different Cu species. Although ionic Cu is known to cause oxidative stress,[31] this mechanism does not predominate for ionic Cu at the concentrations studied herein. By contrast, cells treated with particulate forms of Cu (both nanosized and microsized) exhibited significant ROS production even at the low Cu concentrations studied herein. Our observation suggests that n-Cu provokes a particularly strong biotic ROS response, even at these low concentrations, and is consistent with prior reports that Cu NPs lead to greater cellular oxidative stress in bacterial cells,[32] yeast cells,[33] and mammalian cells[34] than does ionic Cu. Our finding that, out of the species studied, only ionic Cu severely disrupts membrane potential is consistent with a previous study showing that ionic Cu promotes proton leakage across the plasma membrane and hinders the respiratory chain downstream of coenzyme Q.[35] These results highlight important differences in the mechanistic pathways of toxicity for Cu NPs and Cu ions.

Different Cu Species Also Result in Different Types of DNA Damage *in Vitro*. A previous study had demonstrated that ionic Cu, CuO nanoparticles, and microsized CuO particles all result in single-stranded DNA damage,[17] but we wished to explore here if *other* types of DNA damage were caused by the different Cu species studied herein. To study the intrinsic potential of the different Cu species to damage double-stranded DNA, we used a plasmid-based *in vitro* DNA damage assay.[36] In this experiment, the plasmid pUC19 (where 90% of the plasmid is supercoiled and 10% is in single-strand nicked form as purchased)[37] was incubated with each of the Cu species for 24 h; the resulting state of the plasmid was assayed by gel electrophoresis. The gel electrophoresis results for each Cu species are shown in Figure 2A. The positive controls used in this study were a UV-treated plasmid (lane 2 in Figure 2A, which completed degrades the DNA and appears as smeared band) and plasmid treated with the restriction enzyme *Pst*I, (lane 3 in Figure 2A), which results in double strand breaks and hence appears as a linearized plasmid. The DNA damage was classified into linearized DNA (plasmid DNA with a double-strand break), single-stranded, nicked DNA (plasmid DNA with single strand breaks), and fragmented DNA (plasmid DNA with multiple strand breaks). All of the Cu species tested resulted in some form of DNA damage, but the nature and the severity of the damage varied significantly from one Cu species to the next. The most severe DNA damage observed for n-Cu and m-Cu, both of which induced complete degradation of plasmid DNA, resulted in smeared bands at lower molecular weights (Figure 2A). By contrast, both forms of n-$Cu(OH)_2$ (CuPro and Kocide) resulted in complete conversion of the native form of the supercoiled plasmid to open circular (single-strand breaks) and linearized plasmid (double-strand breaks). The remaining Cu species tested (n-CuO, m-CuO and ionic Cu) resulted in partial conversion of the supercoiled DNA to open circular and linearized plasmid.

To test whether the ability of the Cu species to cause DNA damage *in vitro* is linked to the ability of the

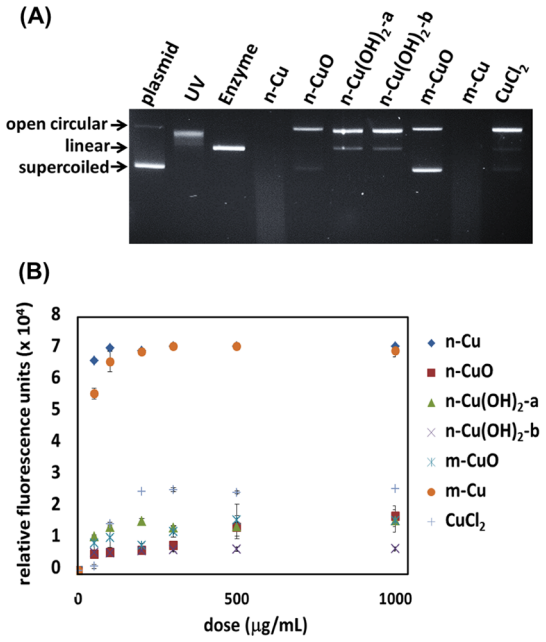

Figure 2. Results from DNA damage assay and abiotic ROS generation. (A) The plasmid pUC19 was treated with the different Cu species for 24 h, and the resulting DNA species were separated and analyzed using gel electrophoresis. UV and restriction enzyme (*Pst*I) were used as positive controls for fragmented and linearized DNA, respectively. Electrophoresis was run at 5 V/cm for 1 h. n-Cu and m-Cu generated the most severe DNA damage and resulted in complete degradation of the plasmid DNA. n-Cu(OH)$_2$-a and n-Cu(OH)$_2$-b induced complete conversion of supercoiled DNA to open circular and linear DNA, while exposure to the other Cu species resulted in only partial conversion of the plasmid DNA. (B) The capability of each particle to generate reactive oxygen species (ROS) was tested *in vitro* using (2′,7′-dichlorofluorescein) DCFH. The particles were treated with DCFH for 2 h and the fluorescence intensity, which reflects the extent of oxidation, was measured using excitation/emission wavelengths of 530/630 nm. Three replicates were performed at each concentration of Cu species.

various species to generate ROS abiotically, (*i.e.*, in the absence of cells), we studied each of the particles using an abiotic ROS generation assay using dichlorodihydro-fluorescein diacetate (DCFH). In this assay, DCFH is generated *in situ* by cleaving the acetate functional group from H_2DCFDA using NaOH.[38] The solution containing DCFH was mixed with each of the Cu species, and the fluorescent signal at 530 nm, which indicates the amount of oxidized dye, was measured after 2 h.[38] A detailed description of the method used for abiotic ROS generation is also provided in the Supplemental Materials and Methods section within the Supporting Information. Only n-Cu and m-Cu, the same two of the particles that resulted in complete DNA degradation, resulted in significant oxidation of DCFH *in vitro* (Figure 2B). This result strongly suggests that the Cu species studied herein that cause significant DNA damage do so by means of DNA oxidation. This result is consistent with previous findings in mammalian cells that nanoparticles induce single/double stranded DNA breaks as well as chromosomal damage using micronucleus, comet and γ-H_2AX assays.[39]

Cellular Imaging Studies Reveal That Cu Nanoparticles Enter the Bacterial Cells Intact. The observation that both n-Cu and m-Cu generate significant ROS under abiotic condition and exhibit significant DNA-damage potential *in vitro*, while n-Cu exhibits significantly higher toxicity toward bacterial cells begs the question of whether there is a difference in the ability of the two particles to enter the bacterial cells and, hence, have direct access to intracellular DNA. To address this question, we examined TEM images of *E. coli* exposed to each of the different Cu species. For these experiments, we chose to focus on *E. coli* because it is a well characterized bacterium and has been used previously to study uptake of nanoparticles.[40,41] To ensure that particles loosely associated with the bacteria were removed, the samples were washed with PBS 3 times prior to obtaining the images. As shown in Figure 3, *E. coli* treated with nanosized particles (n-Cu, n-CuO, n-Cu(OH)$_2$-a and n-Cu(OH)$_2$-b) were observed to have particles-associated with them. By contrast, no Cu particles were observed in cells treated with microsized particles (m-Cu and m-CuO). Interestingly, n-Cu(OH)$_2$-a, n-Cu(OH)$_2$-b and $CuCl_2$-treated bacteria showed a marked distorted conformation of the cells, as well as membrane damage.

To ascertain whether the particles were actually inside the cells, we constructed 3D images of *E. coli* treated with n-Cu from a tomogram series. The resulting image (Figure 4) revealed n-Cu particles inside of the *E. coli*, suggesting that the nanoparticles were able to cross the cell membrane intact. Consistent with the results presented herein, Kumar *et al.* have previously reported the direct uptake of nanoparticles (ZnO and TiO_2) in the bacteria *E. coli*, which they assessed using flow cytometry.[40] Although *E. coli* does not have endocytotic machinery, it is possible that nanoparticles could enter the bacterial cells intact. Results from this study and Rastogi *et al.* demonstrate that Cu NPs lead to membrane damage and the cytoplasmic leakage in *E. coli*,[42] which might permit the internalization of the nanoparticles into the bacterial cells. This result supports the hypothesis that n-Cu can penetrate into the cells, and mediate toxicity through effects of the nanoparticle surface (*e.g.*, DNA damage) in addition to toxicity due to release of Cu ions. In addition, we conducted confocal imaging of both *E. coli* and *L. brevis* that were stained with Hoechst fluorescent dye (which stains nucleic acids inside the cells blue) and treated with n-CuO labeled with FITC (fluorescent green).[43] In both cases, we observed colocalization of the n-FITC-CuO and Hoechst signals. (Supporting Information Figure S8) The results indicate that n-CuO is able to be internalized in both of the species of bacteria studied herein. Taken together, these findings help to explain why we observed both a greater magnitude of toxicity and different mechanisms of toxicity for nano

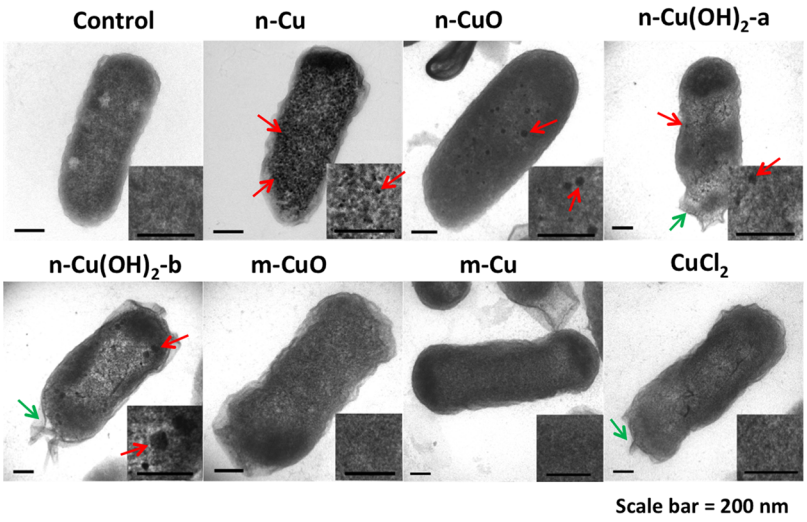

Figure 3. TEM images of *E. coli* cells treated with Cu species. Cells were treated with 0.1 mg/mL of the Cu particles for 24 h before being washed, embedded in resin, and negatively stained before being imaged by TEM. Red arrows indicate Cu particles; green arrows indicate membrane damage. Particles-associated with cells were observed in cells treated with nanosized particles (n-Cu, n-CuO, n-Cu(OH)$_2$-a and n-Cu(OH)$_2$-b).

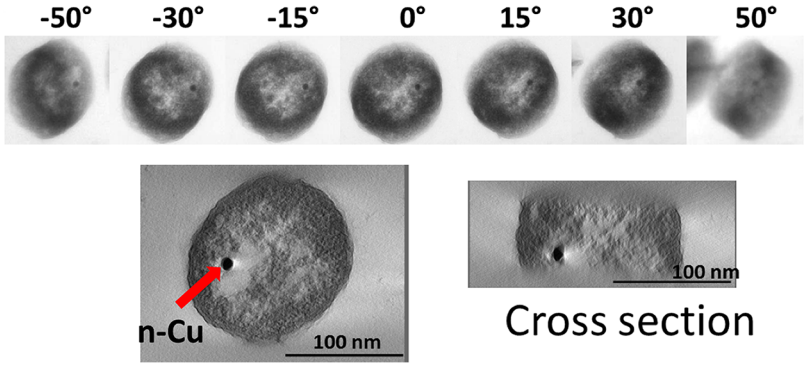

Figure 4. Electron tomography 3D construction reveals the presence of intact Cu nanoparticles inside *E. coli* cells. Cells were treated with 0.1 mg/mL of n-Cu for 24 h before being embedded in the resin, sectioned, and stained (see Materials and Methods). A tilt series of 141 images was recorded by tilting the sample 1° at a time from −70° to +70° and used to construct a 3D tomogram of the sectioned cell. Example images in the tilt series (top panel) and two orthogonal slabs in the 3D tomogram are shown in the bottom panel, showing a single nanoparticle inside the cell (black dot).

Cu species compared with their micrometer and ionic analogues.

CONCLUSIONS

The studies reported herein provide strong evidence that nanosized Cu particles can not only be more toxic than their microsized analogues, but can also exhibit significantly different mechanisms of toxicity than both ionic Cu and microsized Cu. Critically, we found that only nano Cu species were either strongly bound to or internalized within *E. coli* and demonstrated that both n-Cu and n-CuO can be internalized into the bacteria intact. Because n-Cu was also found to generate significant ROS and cause extremely deleterious damage to DNA *in vitro*, the potential that n-Cu may exhibit unique genotoxicity inside cells is particularly of concern. Taken together, these studies suggest that additional safety testing should be conducted on nano Cu species in other organisms.

MATERIALS AND METHODS

Bacterial Strains. Two bacterial strains were used in this study: *E. coli* strain ATCC 25922, a standard strain widely used for antimicrobial disk susceptibility tests, and *L. brevis* strain (Orla-Jensen) ATCC 14869. Chemicals and media components used in these studies are detailed in the Supplemental Materials and Methods section of the Supporting Information.

Physiochemical Characterization of Copper Species. The copper species tested herein were obtained from a variety of sources as described in Supporting Information Table S1. Filtered deionized water was used to make stock solution at 20 mg/mL. Dynamic light scattering (DLS, ZetaPALS, Brookhaven Instruments Ltd., U.K.) was utilized to analyze the average size and size distribution of copper species (50 μg/mL) in water, *E. coli* media (MMD), and *L. brevis* media (Lactobacilli MRS broth). The ζ-potential values of each Cu species in aqueous solution were determined using a ZetaPALS Zeta Potential Analyzer (Brookhaven Instruments Ltd., U.K.). Transmission Electron

Microscopy (TEM) was used to determine the primary size and morphology of the particles. To prepare samples for TEM, a drop of each Cu species in purified water was applied to carbon-coated TEM grids and evaporated at room temperature. Images were taken with a JEOL 1200 EX TEM microscope.

The percent dissolution of each of the Cu species in water and bacterial media was measured by quantifying dissolved Cu by ICP-OES (ICPE-9000 plasma atomic emission spectrometer, Shimadzu). For the analysis, 1 mg/mL of Cu species was suspended in water or bacterial growth media to yield a final volume of 1 mL for 24 h and then was centrifuged at 15 000 rpm for 30 min to precipitate any remaining particles. The supernatant was collected and transferred to a clean tube for acid digestion. Ten milliliters of nitric acid (HNO_3, 65−70%, Trace Metal grade) was added to the supernatant before incubating in a HotBlock (SC100, Environmental Express) at 80 °C for 6 h. The temperature was then raised to 95 °C overnight to evaporate all liquid present in sample. The dried sample was allowed to cool down at room temperature before being dissolved in 2% (v/v) nitric acid at 80 °C for 3 h. The extract was transferred to a 15 mL ICP-OES analysis tube to measure Cu ion concentration.

Growth Inhibition Effects and IC_{50} Calculation. To assess the half-maximal inhibitory concentrations (IC_{50}), a growth inhibition curve was constructed for each Cu species. A 20 mg/mL stock of Cu species was diluted to 10 mg/mL with 2× media (MMD for *E. coli* and Lactobacilli MRS broth for *L. brevis*). Humic acid was added to MMD media as a dispersing agent and was chosen because of its relevance for environmental systems. In this experiment, humic acid (HA) was added to a final concentration of 0.01 mg/mL, and then the resulting mixture was sonicated in water bath (Branson 2510, Danbury, CT) for 15 min at room temperature. Then, 10 mg/mL of each Cu species was then diluted with 1× media supplemented with 0.01 mg/mL HA to a stepwise concentration gradient at 2, 3.9, 7.8, 15.6, 31.3, 62.5, 125, and 250 mg/mL. A total of 50 μL of NP at each concentration was pipetted into 384-well polystyrene microplates. Nine replicates were performed for each concentration. In a separate plate, 50 μL of a log-phase bacterial culture (OD_{600} between 0.5−0.7) was pipetted into the 384-well plate, and then a plastic 384 pin replicator (Genetix Molecular Devices) was used to inoculate bacteria from this plate to the plate containing the serial dilution of Cu species. Sterility and blank controls (bacterial media with no inoculation) were also included for each concentration. A Biotek Synergy plate reader (BioTek, Winooski, VT) was used to monitor OD_{600} every 30 min at 37 °C for 24 h. A growth curve was constructed using the following equation:

$$\text{Growth } (\%) = \frac{A_{\text{Np, B}} - A_{\text{Np, A}}}{A_{\text{Bl, B}} - A_{\text{Bl, A}}} \times 100$$

In the above equation, $A_{\text{Np,B}}$ is the absorbance of the bacterial culture in the presence of each concentration of Cu NPs (average of 9 replicates); $A_{\text{Np,A}}$ is the absorbance of the Cu NPs at the respective concentrations which contain no bacteria (average of 3 replicates); $A_{\text{Bl,B}}$ is the absorbance of the bacterial culture in blank (no Cu species) media (average of 9 replicates), and $A_{\text{Bl,B}}$ is the absorbance of media with no bacteria (average of 3 replicates). The growth inhibition curve was plotted using the program Origin version 9 (OriginLab Corporation) using the category Growth/Sigmoidal, function Logistic. The IC_{50} and standard error were calculated for each data set using the same program.

***In Vitro* Assays.** *In Vitro DNA Damage Assay.* Purified plasmid pUC19 (Thermo Scientific, catalog #SD0061) was incubated in the presence of 100 mg/L Cu species for 24 h in purified water. Centrifugation at 15 000 rpm for 30 min was used to separate plasmid DNA from residual Cu NPs. The supernatant containing the plasmid DNA was collected and loaded into a 1.2% Tris−acetate EDTA buffer, TAE agarose gel. Electrophoresis was performed at 5 V/cm for 1 h and the resulting gel was stained with ethidium bromide for 30 min. A Bio-Rad FX imaging system was used to image the gel; the band intensities were quantified using QuantityOne software. To linearize the pUC19 (first positive control), the restriction enzyme, *Pst*I was incubated with the plasmid at 37 °C for 1 h. To induce random nicking and DNA fragmentation (second positive control), the plasmid was treated with a xenon arc UV-B lamp (Asahi Spectra, LAX-Cute) for 10 min at 1000 mJ/cm^2. For the negative control, pUC19 was loaded into the electrophoresis gel, whereas the majority of the plasmid as purchased was in the supercoiled-formed of DNA.

Determining Cell-Associated Cu Using Sucrose Gradient Centrifugation and ICP-OES. *E. coli* and *L. brevis* were treated with 0.5 and 1 mg/L of a series of the Cu species. After 24 h, the cells were washed 2 times with PBS, and then sucrose gradient centrifugation was used to separate the cells from residual particulate Cu. To make the sucrose gradient, 0.3, 0.4, and 0.6 g/mL of sucrose (Sigma-Aldrich) were completely dissolved in water and filtered with a 0.22 μm Millipore filter.[44] A volume of 1.2 mL of each sucrose concentration was carefully layered into a 15 mL Falcon tube, and then 1 mL of cell suspension was placed on top of the gradient. The mixture was centrifuged (Eppendorf 5810 R) at 2916*g* for 5 min at room temperature. After centrifugation, a brown band of cells was clearly visible at the upper part of the gradient, and Cu species were visibly precipitated at the bottom of the tube (see Supporting Information Figure S5). A total of 1.2 mL of cells suspension was collected. To determine the total number of bacterial cells, a standard curve between OD_{600} and the number of cells was constructed (Supporting Information Figure S6, (A) for *E. coli* and (B) for *L. brevis*). The total amount of cell-associated Cu was normalized as the Cu content per 10^9 cells for each bacterial species. The number of cells was determined by measuring the OD_{600} of 200 μL of this suspension. To determine the amount of cell-associated copper, 1 mL of the suspension was digested with 10 mL of pure HNO_3 overnight and then was evaporated at 95 °C until no liquid remained. Two percent HNO_3 was used to resuspend the sample. Cu content was analyzed using ICP-OES (ICPE-9000, Shimadzu).

Determining Bioavailable, Intracellular Cu with Biosensor Strain of *E. coli*. The amount of bioavailable, intracellular Cu was determined using a genetically engineered *E. coli* biosensor strain in which bioluminescence specifically responds to Cu cellular bioavailability (MC1061 pSLcueR/pDNPcopAlux, "Cu-inducible strain"). The luminescent strain was constructed as previously described in Bondarenko *et al.*[17] A colony of the bacteria was inoculated into 3 mL of fresh LB media supplemented with 100 mg/L ampicillin and allowed to grow overnight before being diluted 1:50 using fresh LB media with antibiotic. The culture was allowed to grow to reach log phase (OD_{600} of 0.6) before the cells were harvested for the experiment. Growth was conducted at 30 °C, shaking at 200 rpm. Twenty-five microliters of the Cu species in MMD supplemented with 0.01 mg/mL humic acid was mixed with 25 μL of the biosensor bacteria in a 384-well plate to yield a final bacterial OD_{600} of 0.1. The plate was kept at 30 °C for 2 h to allow for luminescence induction, at which point the luminescence was quantified using a microplate reader (SpectraMax MS, Molecular Devices, Sunnyvale, CA).

Microscopy of Bacterial Cells Exposed to Cu Species. *TEM Sample Preparation and Microscopy. E. coli* cells that had been treated with 0.1 mg/mL Cu species for 24 h were washed 3 times with phosphate-buffered saline (PBS) before being fixed with 2% glutaraldehyde in 0.1 M PBS. Cells were washed with PBS 3 times before treating with osmium tetroxide (OsO_4) in PBS for 1 h. After rinsing 3 times with PBS, the cell pellet was dehydrated in a graded series of ethanol (30%, 50%, 70%, 80%, 90%, 95%, and 100% ethanol for 2 h each). Propylene oxide was used to remove any residual ethanol before the pellet was embedded in Epon resin (Sigma-Aldrich). A Reichert-Jung Ultracut E ultramicrotome was used to cut 100 nm thick sections which were placed onto 1GG200 gold grids (Ted Pell, Inc.). Sections were stained with uranyl acetate and Reynolds lead citrate, and examined on an FEI T12 transmission electron microscope operated at 80 kV in the Electron Imaging Center for Nanomachines (EICN) at UCLA.

Electron Tomography and 3D Reconstruction. E. coli cells that had been treated with Cu NPs for 24 h were washed, dehydrated and embedded in Epon resin as described above. A Reichert-Jung Ultracut E ultramicrotome was used to make

250 nm thick sections from the block, which were placed onto Maxtaform 75/300 Rectangular Mesh copper grids (Ted Pell, Inc.). An FEI Tecnai F20 transmission electron microscope was used to capture the tomography tilt series. A Gatan 626 cryo specimen holder was used to collect images in tilt angles ranging from −70° to +70°, with a 1° increment. The tilt series of 141 images were used to reconstruct 3D volumes using the Etomo tomography processing software in the Imod package (Boulder Laboratory for 3-D Electron Microscopy of Cells).[45]

Confocal Microscopy. *E. coli* and *L. brevis* were treated with 50 mg/L of n-FITC-CuO for 24 h before being washed 3 times with PBS. The bacteria were fixed using 4% paraformaldehyde for 20 min at room temperature. After another 3 washes with PBS, the cells were stained with Hoechst 33342, which specifically stains bacterial DNA, yielding blue fluorescence. After 1 h of incubation with Hoechst dye, the cells were washed 3 times and placed into an 8-well chamber slide (Lab Tek) before being visualized under a confocal microscope (Leica Confocal SP2 1P/FCS). For Hoechst dye, the excitation wavelength used was 358 nm, and E_{max} was monitored at 420−500 nm. For FITC, the excitation wavelength used was 488 nm, and E_{max} was monitored at 520−580 nm.

Safe Handling of Nanomaterials. Nanoparticles as dry powders were handled in a chemical fume hood or powder enclosure, and manipulated while the researcher was wearing a N95 filer mask. After suspension in aqueous solutions, standard good chemical hygiene practices were employed. Sonication can result in aerolization and thus was only performed on solutions that were in closed containers. More detailed recommendations are available in the *Nanotoolkit* developed by the *California Nanosafety Consortium of Higher Education* which is available online at: http://www.cein.ucla.edu/new/p155.php.

Conflict of Interest: The authors declare no competing financial interest.

Acknowledgment. This study was performed at the University of California Center for Environmental Implications of Nanotechnology (UC CEIN). We wish to acknowledge the Electron Imaging Center for NanoMachines (EICN, supported by NIH 1S10RR23057 to Z. H. Zhou) of the California Nanosystems Institute and the Electron Microscope Services Center of Brain Research Institute. C. Kaweeteerawat was supported financially by the Royal Thai government. This material is based upon work supported by the UC CEIN through a grant from the National Science Foundation and the Environmental Protection Agency under Cooperative Agreement Numbers DBI-0830117 and DBI-12266377. The paper has not been subjected to the U.S. Environmental Protection Agency's internal review; therefore, the opinions expressed in this paper are those of the author(s) and do not, necessarily, reflect the official positions and policies of the U.S. EPA.

Supporting Information Available: Additional details relate to Supplemental Materials and Methods, growth inhibition effects of Cu species in *E. coli* and *L. brevis* (Figure S1), individual growth inhibition curve including error bars for each of the Cu species in *E. coli* and *L. brevis* (Figure S2), area under growth-inhibition curve for Cu species in *E. coli* and *L. brevis* (Figure S3), comparison of regression lines for area under the growth inhibition curve as a function of % Cu dissolved in media for *E. coli* and *L. brevis* (Figure S4), schematic of sucrose gradient centrifugation procedure (Figure S5), standard curve of OD_{600} and total number of cells (Figure S6), Cu bioavailability determined using bacterial biosensor strain (Figure S7), and confocal images of cells treated with n-FITC-CuO (Figure S8). Tables of data include: sources of Cu particles (Table S1), correlation coefficients for area under the growth inhibition curve and amounts of dissolved copper in media, cell-associated Cu, and Cu bioavailable in each of the bacterial species (Table S2), correlation between results from growth inhibition assays and results from the suite of sublethal assays (Table S3), and References for Supporting Information. The Supporting Information is available free of charge on the ACS Publications website at DOI: 10.1021/acsnano.5b02021.

REFERENCES AND NOTES

1. National Nanotechonology Initiative: http://www.nano.gov/you/nanotechnology-benefits (accessed May 31, 2015).
2. Pham, L. Q.; Sohn, J. H.; Kim, C. W.; Park, J. H.; Kang, H. S.; Lee, B. C.; Kang, Y. S. Copper Nanoparticles Incorporated With Conducting Polymer: Effects of Copper Concentration and Surfactants on the Stability and Conductivity. *J. Colloid Interface Sci.* **2012**, *365*, 103–109.
3. Saterlie, M.; Sahin, H.; Kavlicoglu, B.; Liu, Y. M.; Graeve, O. Particle Size Effects in the Thermal Conductivity Enhancement of Copper-Based Nanofluids. *Nanoscale Res. Lett.* **2011**, *6*, 217–223.
4. Almeida, E.; Diamantino, T. C.; de Sousa, O. Marine Paints: The Particular Case of Antifouling Paints. *Prog. Org. Coat.* **2007**, *59*, 2–20.
5. Ren, G. G.; Hu, D. W.; Cheng, E. W. C.; Vargas-Reus, M. A.; Reip, P.; Allaker, R. P. Characterisation of Copper Oxide Nanoparticles for Antimicrobial Applications. *Int. J. Antimicrob. Agents* **2009**, *33*, 587–590.
6. Melegari, S. P.; Perreault, F.; Costa, R. H. R.; Popovic, R.; Matias, W. G. Evaluation of Toxicity and Oxidative Stress Induced by Copper Oxide Nanoparticles in the Green Alga *Chlamydomonas reinhardtii*. *Aquat. Toxicol.* **2013**, *142-143*, 431–440.
7. Mwaanga, P.; Carraway, E. R.; van den Hurk, P. The Induction of Biochemical Changes in *Daphnia magna* by CuO and ZnO Nanoparticles. *Aquat. Toxicol.* **2014**, *150*, 201–9.
8. Gomes, T.; Pinheiro, J. P.; Cancio, I.; Pereira, C. G.; Cardoso, C.; Bebianno, M. J. Effects of Copper Nanoparticles Exposure in the Mussel *Mytilus galloprovincialis*. *Environ. Sci. Technol.* **2011**, *45*, 9356–62.
9. Griffitt, R. J.; Weil, R.; Hyndman, K. A.; Denslow, N. D.; Powers, K.; Taylor, D.; Barber, D. S. Exposure to Copper Nanoparticles Causes Gill Injury and Acute Lethality in Zebrafish (*Danio rerio*). *Environ. Sci. Technol.* **2007**, *41*, 8178–86.
10. Dasari, T. P.; Pathakoti, K.; Hwang, H. M. Determination of the Mechanism of Photoinduced Toxicity of Selected Metal Oxide Nanoparticles (ZnO, CuO, $Co3O_4$ and TiO_2) to *E. coli* Bacteria. *J. Environ. Sci.* **2013**, *25*, 882–888.
11. Mancuso, L.; Cao, G. Acute Toxicity Test of CuO Nanoparticles Using Human Mesenchymal Stem Cells. *Toxicol. Mech. Methods* **2014**, *24*, 449–54.
12. Zhang, H. Y.; Ji, Z. X.; Xia, T.; Meng, H.; Low-Kam, C.; Liu, R.; Pokhrel, S.; Lin, S. J.; Wang, X.; Liao, Y. P.; et al. Use of Metal Oxide Nanoparticle Band Gap to Develop a Predictive Paradigm for Oxidative Stress and Acute Pulmonary Inflammation. *ACS Nano* **2012**, *6*, 4349–4368.
13. Xiu, Z. M.; Zhang, Q. B.; Puppala, H. L.; Colvin, V. L.; Alvarez, P. J. Negligible Particle-Specific Antibacterial Activity of Silver Nanoparticles. *Nano Lett.* **2012**, *12*, 4271–5.
14. McQuillan, J. S.; Shaw, A. M. Differential Gene Regulation in the Ag Nanoparticle and Ag(+)-Induced Silver Stress Response in *Escherichia coli*: A Full Transcriptomic Profile. *Nanotoxicology* **2014**, *8*, 177–84.
15. Ivask, A.; Elbadawy, A.; Kaweeteerawat, C.; Boren, D.; Fischer, H.; Ji, Z.; Chang, C. H.; Liu, R.; Tolaymat, T.; Telesca, D.; et al. Toxicity Mechanisms in *Escherichia coli* Vary for Silver Nanoparticles and Differ from Ionic Silver. *ACS Nano* **2014**, *8*, 374–86.
16. Wang, Z.; Liu, S.; Ma, J.; Qu, G.; Wang, X.; Yu, S.; He, J.; Liu, J.; Xia, T.; Jiang, G. B. Silver Nanoparticles Induced RNA Polymerase-Silver Binding and RNA Transcription Inhibition in Erythroid Progenitor Cells. *ACS Nano* **2013**, *7*, 4171–86.
17. Bondarenko, O.; Ivask, A.; Kakinen, A.; Kahru, A. Sub-Toxic Effects of CuO Nanoparticles on Bacteria: Kinetics, Role of Cu Ions and Possible Mechanisms of Action. *Environ. Pollut.* **2012**, *169*, 81–9.
18. Dimkpa, C. O.; McLean, J. E.; Britt, D. W.; Johnson, W. P.; Arey, B.; Lea, A. S.; Anderson, A. J. Nanospecific Inhibition of Pyoverdine Siderophore Production in *Pseudomonas chlororaphis* O6 by CuO Nanoparticles. *Chem. Res. Toxicol.* **2012**, *25*, 1066–74.

19. Rossetto, A. L.; Melegari, S. P.; Ouriques, L. C.; Matias, W. G. Comparative Evaluation of Acute and Chronic Toxicities of CuO Nanoparticles and Bulk Using *Daphnia magna* and *Vibrio fischeri*. *Sci. Total Environ.* **2014**, *490*, 807–14.
20. Adeleye, A. S.; Conway, J. R.; Perez, T.; Rutten, P.; Keller, A. A. Influence of Extracellular Polymeric Substances on the Long-Term Fate, Dissolution, and Speciation of Copper-Based Nanoparticles. *Environ. Sci. Technol.* **2014**, *48*, 12561–8.
21. Lin, S. J.; Taylor, A. A.; Ji, Z. X.; Chang, C. H.; Kinsinger, N. M.; Ueng, W.; Walker, S. L.; Nel, A. E. Understanding the Transformation, Speciation, and Hazard Potential of Copper Particles in a Model Septic Tank System Using Zebrafish to Monitor the Effluent. *ACS Nano* **2015**, *9*, 2038–2048.
22. Kato, H.; Fujita, K.; Horie, M.; Suzuki, M.; Nakamura, A.; Endoh, S.; Yoshida, Y.; Iwahashi, H.; Takahashi, K.; Kinugasa, S. Dispersion Characteristics of Various Metal Oxide Secondary Nanoparticles in Culture Medium for *In Vitro* Toxicology Assessment. *Toxicol. In Vitro* **2010**, *24*, 1009–1018.
23. Andreazza, R.; Okeke, B. C.; Pieniz, S.; Bento, F. M.; Camargo, F. A. O. Biosorption and Bioreduction of Copper from Different Copper Compounds in Aqueous Solution. *Biol. Trace Elem. Res.* **2013**, *152* (3), 411–416.
24. Szymonska, J.; Wieczorek, J.; Molenda, M.; Bielanska, E. Uptake of Cu^{2+} by Starch Granules as Affected by Counterions. *J. Agric. Food Chem.* **2008**, *56* (11), 4054–4059.
25. United Nations. *Globally Harmonized System for the Classification and Labelling of Chemicals*, 5th Revised Edition; UN: New York and Geneva, **2013**. http://www.unece.org/fileadmin/DAM/trans/danger/publi/ghs/ghs_rev05/English/ST-SG-AC10-30-Rev5e.pdf.
26. Haggstrom, J. A.; Klabunde, K. J.; Marchin, G. L. Biocidal Properties of Metal Oxide Nanoparticles and Their Halogen Adducts. *Nanoscale* **2010**, *2*, 399–405.
27. Azam, A.; Ahmed, A. S.; Oves, M.; Khan, M. S.; Habib, S. S.; Memic, A. Antimicrobial Activity of Metal Oxide Nanoparticles Against Gram-positive and Gram-negative Bacteria: a Comparative Study. *Int. J. Nanomed.* **2012**, *7*, 6003–9.
28. Gaber, M.; El-Ghamry, H. A.; Fathalla, S. K. Ni(II), Pd(II) and Pt(II) Complexes of (1H-1,2,4-triazole-3-ylimino)methyl]-naphthalene-2-ol. Structural, Spectroscopic, Biological, Cytotoxicity, Antioxidant and DNA Binding. *Spectrochim. Acta, Part A* **2015**, *139*, 396–404.
29. Lo Giudice, A.; Casella, P.; Bruni, V.; Michaud, L. Response of Bacterial Isolates From Antarctic Shallow Sediments Towards Heavy Metals, Antibiotics and Polychlorinated Biphenyls. *Ecotoxicology* **2013**, *22*, 240–50.
30. Taylor, R. Interpretation of the Correlation-Coefficient - A Basic Review. *J. Diagn. Med. Sonog.* **1990**, *6*, 35–39.
31. Gaetke, L. M.; Chow, C. K. Copper Toxicity, Oxidative Stress, and Antioxidant Nutrients. *Toxicology* **2003**, *189*, 147–163.
32. Li, F.; Lei, C.; Shen, Q.; Li, L.; Wang, M.; Guo, M.; Huang, Y.; Nie, Z.; Yao, S. Analysis of Copper Nanoparticles Toxicity Based on a Stress-Responsive Bacterial Biosensor Array. *Nanoscale* **2013**, *5*, 653–62.
33. Kasemets, K.; Suppi, S.; Kunnis-Beres, K.; Kahru, A. Toxicity of CuO Nanoparticles to Yeast *Saccharomyces cerevisiae* BY4741 Wild-Type and Its Nine Isogenic Single-Gene Deletion Mutants. *Chem. Res. Toxicol.* **2013**, *26*, 356–67.
34. Liu, Y.; Gao, Y.; Liu, Y.; Li, B.; Chen, C.; Wu, G. Oxidative Stress and Acute Changes in Murine Brain Tissues After Nasal Instillation of Copper Particles With Different Sizes. *J. Nanosci. Nanotechnol.* **2014**, *14*, 4534–40.
35. Ciapaite, J.; Nauciene, Z.; Baniene, R.; Wagner, M. J.; Krab, K.; Mildaziene, V. Modular Kinetic Analysis Reveals Differences in Cd^{2+} and Cu^{2+} Ion-Induced Impairment of Oxidative Phosphorylation in Liver. *FEBS J.* **2009**, *276*, 3656–68.
36. Leba, L. J.; Brunschwig, C.; Saout, M.; Martial, K.; Vulcain, E.; Bereau, D.; Robinson, J. C. Optimization of a DNA Nicking Assay to Evaluate *Oenocarpus bataua* and *Camellia sinensis* Antioxidant Capacity. *Int. J. Mol. Sci.* **2014**, *15*, 18023–39.
37. https://www.lifetechnologies.com/order/catalog/product/SD0061?lCID=search-product (accessed March 9, 2015).
38. Chin, R. M.; Fu, X.; Pai, M. Y.; Vergnes, L.; Hwang, H.; Deng, G.; Diep, S.; Lomenick, B.; Meli, V. S.; Monsalve, G. C.; et al. The Metabolite Alpha-Ketoglutarate Extends Lifespan by Inhibiting ATP Synthase and TOR. *Nature* **2014**, *510*, 397–401.
39. Kumbicak, U.; Cavas, T.; Cinkilic, N.; Kumbicak, Z.; Vatan, O.; Yilmaz, D. Evaluation of *In Vitro* Cytotoxicity and Genotoxicity of Copper-Zinc Alloy Nanoparticles in Human Lung Epithelial Cells. *Food Chem. Toxicol.* **2014**, *73*, 105–112.
40. Kumar, A.; Pandey, A. K.; Singh, S. S.; Shanker, R.; Dhawan, A. A Flow Cytometric Method to Assess Nanoparticle Uptake in Bacteria. *Cytometry, Part A* **2011**, *79*, 707–12.
41. Jayawardena, H. S.; Jayawardana, K. W.; Chen, X.; Yan, M. Maltoheptaose Promotes Nanoparticle Internalization by *Escherichia coli*. *Chem. Commun.* **2013**, *49*, 3034–6.
42. Rastogi, L.; Arunachalam, J. Synthesis and Characterization of Bovine Serum Albumin-Copper Nanocomposites for Antibacterial Applications. *Colloids Surf., B* **2013**, *108*, 134–41.
43. Li, R.; Ji, Z.; Chang, C. H.; Dunphy, D. R.; Cai, X.; Meng, H.; Zhang, H.; Sun, B.; Wang, X.; Dong, J.; et al. Surface Interactions With Compartmentalized Cellular Phosphates Explain Rare Earth Oxide Nanoparticle Hazard and Provide Opportunities for Safer Design. *ACS Nano* **2014**, *8*, 1771–83.
44. Berk, S. G.; Guerry, P.; Colwell, R. R. Separation of Small Ciliate Protozoa From Bacteria by Sucrose Gradient Centrifugation. *Appl. Environ. Microbiol.* **1976**, *31* (3), 450–452.
45. Kremer, J. R.; Mastronarde, D. N.; McIntosh, J. R. Computer Visualization of Three-Dimensional Image Data Using IMOD. *J. Struct. Biol.* **1996**, *116*, 71–76.